

# INVESTIGATION OF COMPRESSIVE BEHAVIOUR OF GLASS/CARBON FIBRE HYBRID COMPOSITE WITH 4-POINT FLEXURAL TEST

Aree Tongloet<sup>1\*</sup>, Xun Wu<sup>2</sup>, Michael R. Wisnom<sup>3</sup>

Bristol Composites Institute, University of Bristol Queen's Building, BS8 1TR, Bristol, United Kingdom, web page: <http://www.bristol.ac.uk/composites/><sup>1</sup>Email: [zl20421@bristol.ac.uk](mailto:zl20421@bristol.ac.uk)

<sup>2</sup>Email: [xunxun.wu@bristol.ac.uk](mailto:xunxun.wu@bristol.ac.uk)

<sup>3</sup>Email: [M.Wisnom@bristol.ac.uk](mailto:M.Wisnom@bristol.ac.uk)

**Keywords:** Hybrid composites, Compression, Knee-point, Pseudo-ductility

## ABSTRACT

Pseudo-ductile stress-strain behaviour of thin-ply hybrid composites has been presented in various studies [1] [2], but the compressive behaviour of glass/thin carbon hybrid composites is still not well understood. Four-point flexural tests on sandwich beams have been chosen to investigate the compressive behaviour of the glass/thin high-modulus carbon hybrid composites in this study and to obtain a baseline compressive failure strain for the carbon fibre composite. The compressive response of 913 S-glass/M55 high-modulus carbon fibre hybrids has been investigated. Gauge section failures on the compression side of the beam have been observed without premature failure such as core shear failure, localised roller failure or tensile failure on the bottom layer.

## 1 INTRODUCTION

The hybrid composite concept has been introduced to improve the strength of carbon fibre composite by hybridising low-strain fibre with higher-strain fibre material [6-7]. Hybrid composite systems with appropriate high modulus, low strain material thickness create pseudo-ductile failure characteristics under tensile loading [7]. Pseudo-ductility of low-strain/high-strain fibre hybrid composites has been studied to improve the performance and mitigate sudden failure including self-monitoring of damage. Suwarta et al. studied the compressive behaviour of 913 S-glass/M55 hybrid composites with different glass/carbon fibre ratios under conventional direct compression [8]. The result with a thin-ply hybrid configuration showed a knee-point on the stress-strain response with pseudo-ductile response due to carbon ply fragmentation. The thicker carbon fibre ply composites showed lower final compressive failure strains due to earlier delamination.

Traditional direct compression tests used to characterise the compressive behaviour of fibre-polymeric composite materials have several problems. The first concern is stress concentrations at the grips during the test and failure initiation from high shear stresses [5,10-11]. 3-point and 4-point flexural tests have been proposed to investigate the compressive behaviour of composite material due to the lower stress concentration that occurs during the test compared to the traditional direct compression procedure [9]. Although flexural tests mitigate the problems from direct compression tests, this experiment setup creates a through-thickness strain gradient and may be susceptible to premature roller failure during the test [9]. To mitigate these limitations, a sandwich beam specimen has been proposed to reduce the through-thickness strain gradient and a large loading roller diameter to avoid the possibility of roller failure [9]. Most studies with sandwich beams are with honeycomb material, but the honeycomb material is susceptible to failure due to low core shear strength, core crushing and debonding, thus the new sandwich specimen with a wooden core has been developed which gives consistent gauge section compressive failures [9].

The objectives of this study are to characterise the compressive behaviour of glass fibre hybridised with high modulus carbon fibre by observing the load-strain response and damage that occurs through

an optical microscope and scanning electron microscope (SEM). Another objective is to study the failure characteristics of hybrid composites to understand the influence of the carbon fibre thickness.

## 2 SPECIMEN DESIGN AND PREPARATION

Sandwich beam specimens in this study are comprised of a hybrid laminate as the top skin, a wooden core and an IM7/8552 laminate as the bottom skin, tested by a bending method developed by Wu and Wisnom [9]. In order to achieve compressive failure in the top skin, the key design drivers for the sandwich beam are avoiding shear failure of the core material, localised failure from the loading rollers and tensile failure of the bottom skin. Both the top skin and bottom skin were cured in an autoclave and bonded to the core with epoxy adhesive with an overnight curing process at room temperature. The top skin consisted of M55/epoxy carbon fibre plies at the centre with one 913 S-glass layer on either side, making the average thickness to be 0.34 mm. 913 S-glass/M55-epoxy hybrid composites were cured in an autoclave with the curing cycle shown in Figure 1.

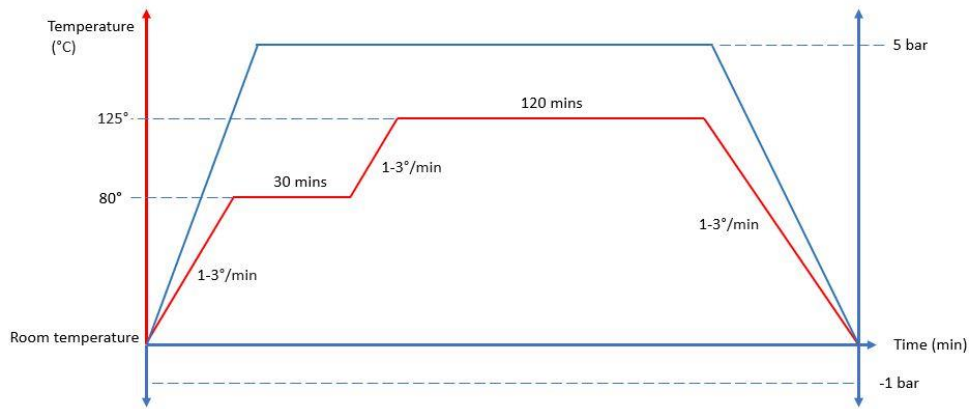


Figure 1: Curing cycle for M55/S-glass 913 hybrid composite

The hybrid composite and IM7/8552 laminates were cut into 25 mm strips along the fibre direction for the sandwich beam manufacturing with a table saw equipped with a diamond-coated blade. Ash wood with 18 mm thickness was selected as the core material because it provides higher shear strength compared to honeycomb material [9]. The wooden beams were cut along the longitudinal grain direction to maximise the strength of the material. To determine the span of the beam, equation (1) from classical beam theory was used to calculate the required bending moment ( $M$ ) on the sandwich beam.

$$M = \frac{\sigma_c I}{cn} \quad (1)$$

Where  $\sigma_c$  is the expected compressive strength of carbon fibre.  $n$  is the proportional value of the hybrid composite's modulus to the modulus of ash wood.  $c$  is the distance from the neutral axis to the top surface of the carbon fibre ply.  $I$  is second moment of area of the sandwich beam. The support span of the beam was calculated from the bending moment with equation (2), see schematic in Figure 2.  $F$  is the applied compressive force from the loading noses which is limited to 5000 N for this study based on previous work on avoiding local failure [9].

$$S = \frac{4M}{F} + L \quad (2)$$

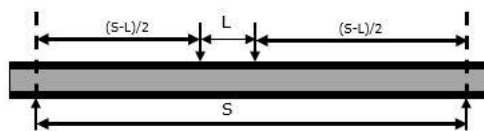


Figure 2: Schematic of the beam for the design

Prepreg type	M55/epoxy <sup>[3][4]</sup>	913 S-glass <sup>[12]</sup>	IM7/8552 <sup>[4]</sup>
Composite modulus (GPa)	280	45.7	164
Cured nominal thickness (mm)	0.03	0.155	0.125
Tensile strain to failure (%)	0.8	3.98 <sup>[10]</sup>	1.6
Compressive strain to failure (%)	-0.46	2.33 <sup>[10]</sup>	-1.16
Poisson ratio	0.25	0.3	0.32
CTE in fibre direction, $\alpha_{11}$ (1/K)	$-1.1 \times 10^{-6}$	$3.8 \times 10^{-6}$	$-4.0 \times 10^{-7}$
CTE in transverse direction, $\alpha_{22}$ (1/K)	$3 \times 10^{-5}$	$2.6 \times 10^{-5}$	$2.5 \times 10^{-5}$

Table 1: Material properties of M55/epoxy, S-glass/913 and IM7/8552 composites

Core thickness (mm)	Modulus of elasticity (GPa) <sup>[13]</sup>	Shear modulus (MPa) <sup>[13]</sup>	Shear strength (MPa) <sup>[14]</sup>
18	8.2	1234	14.3

Table 2: Properties of Ashwood

### 3 EXPERIMENT SETUP AND EQUIPMENT

This study used an Instron 8872 universal testing machine with a hydraulic actuator equipped with a 25kN load cell. A support rig was placed on the machine's base to support the sandwich beam and the span is adjustable to meet the design for a particular hybrid configuration. Loading noses with 25 mm diameter were fixed in the upper jaw of the testing machine and the spacing between the rollers was 40 mm and the outer span of the experiment was 600 mm, as shown in Figure 3.

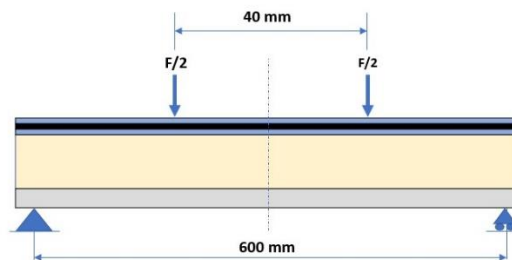


Figure 3: Schematic of the sandwich beam design (not to scale)



Figure 4: Experimental setup for the 4-point flexural test with the sandwich beam.

To measure the strain during the test, linear strain gauges model C4A-06-060SL-350-39P from Vishay were attached on both the top and bottom skin at the centre of the sandwich beam. A static crosshead speed of 2 mm/min was used to apply the compressive load on the sandwich beam until the material reached final failure. The failure of the hybrid composites was characterised by using an optical microscope after the tests, putting the specimens in a resin pot and polishing them.

#### 4 EXPERIMENT RESULT AND DISCUSSION

A typical compressive load-compressive strain response from the  $SG_1/M55_1/SG_1$  sandwich beams under 4-point flexural tests is shown in Figure 5. It exhibited a linear response at the initial stage of the loading, followed by a non-linear response until reaching final failure, with a clear knee point observed. The knee point was determined by the intersection point of two tangential lines. A knee point compressive strain of 0.483% was seen on the load-strain curve and it is called the pseudo-yield point. The hybrid laminate continued to carry load until it debonded from the wooden. The final average failure strain of the material is 0.774%. Small fibre fragmentations have been observed in the central carbon layers, which can be seen as scattered white strips on the top skin across the width and along the length of the sandwich beam as shown in Figure 6. Figure 7 shows the failure of the hybrid composite observed through a Zeiss optical microscope, and there is no evidence of a kink band. The experimental result was similar to the knee point compressive strain of 0.49%, obtained from a similar composite layup tested in direct compression [8]. The experimental result on the hybrid composite was compared to a compressive test by bending on a pure M55 carbon fibre composite beam 2.22 mm thick, where a sudden failure response was seen with 0.31% final failure compressive strain [15]. The current study confirms that the hybrid composite can mitigate the sudden failure of the high modulus carbon fibre and enhance the compressive failure strain of the material.

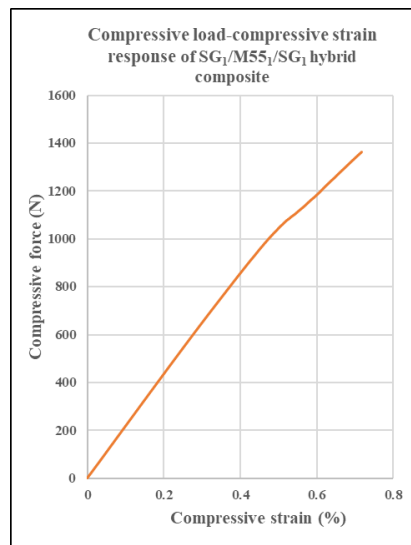


Figure 5: Load-strain response of the  $SG_1/M55_1/SG_1$  hybrid composite

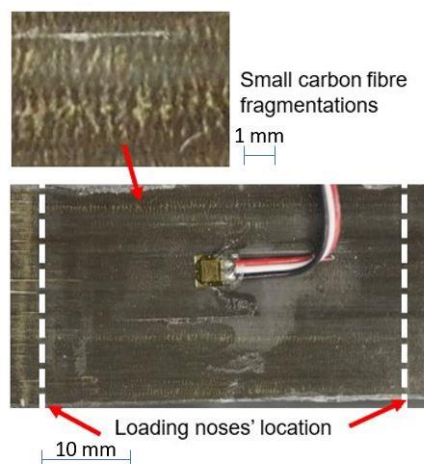


Figure 6: Damage characteristics of the  $SG_1/M55_1/SG_1$  hybrid composites on the top surface of the sandwich beam

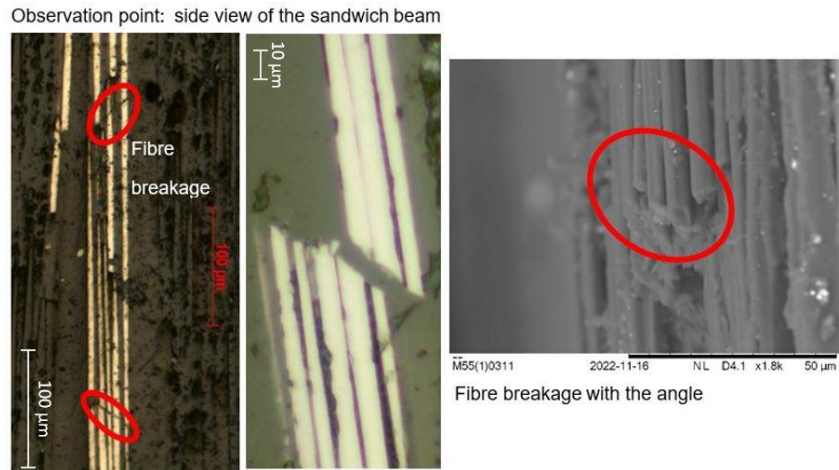


Figure 7: Damage characteristics of the SG<sub>1</sub>/M55<sub>1</sub>/SG<sub>1</sub> hybrid composites observed from the side of the specimen

Specimen configuration	Knee-point compressive strain (%)	Failure compressive strain (%)	Failure compressive force (N)	Failure mode
SG <sub>1</sub> /M55 <sub>1</sub> /SG <sub>1</sub>	0.484 (3)	0.774 (11)	1800 (10)	Small carbon fragmentation

Table 3: Summary of the experimental results from SG<sub>1</sub>/M55<sub>1</sub>/SG<sub>1</sub>. The number in the bracket is coefficient of variation in percentage.

## 5 CONCLUSION

The compressive behaviour of S-glass/thin high modulus carbon hybrid laminate has been investigated using an unconventional sandwich beam in bending. A pseudo-ductile response has been achieved with small carbon fragmentations without catastrophic failure. This experiment that the showed hybridisation concept would be helpful to enhance the compressive behaviour of the material.

## ACKNOWLEDGEMENTS

Aree Tongloet is supported by the Royal Thai Government scholarship provided by the Office of the Civil Service Commission (OCSC), Royal Government of Thailand.

## REFERENCES

- [1] Wisnom MR, Czél G, Swolfs Y, Jalalvand M, Gorbatiikh L, Verpoest I. Hybrid effects in thin ply carbon/glass unidirectional laminates: Accurate experimental determination and prediction. *Compos Part A Appl Sci Manuf* 2016;88:131–9. <https://doi.org/10.1016/j.compositesa.2016.04.014>
- [2] Jalalvand M, Czél G, Wisnom MR. Damage analysis of pseudo-ductile thin-ply UD hybrid composites - A new analytical method. *Compos Part A Appl Sci Manuf* 2015;69:83–93. <https://doi.org/10.1016/j.compositesa.2014.11.006>
- [3] Czél G, Suwarta P, Jalalvand M, Wisnom MR. Investigation of the compression performance and failure mechanism of pseudo-ductile thin-ply hybrid composites. *ICCM Int. Conf. Compos. Mater.*, vol. 2017- Augus, 2017, p. 20–5. <https://www.iccm-central.org/Proceedings/ICCM21proceedings/papers/3889.pdf>
- [4] Wu X, Fuller JD, Wisnom MR. Role of fibre fragmentation on pseudo-ductility of thin-ply [ $\pm 27/0$ ]s carbon fibre laminates with high modulus 0° plies under compressive and flexural loading. *Compos Sci Technol* 2020;199:108377. <https://doi.org/10.1016/j.compscitech.2020.108377>
- [5] Swolfs Y, Gorbatiikh L, Verpoest I. Fibre hybridisation in polymer composites: A review.

- Compos Part A Appl Sci Manuf 2014;67:181–200.  
<https://doi.org/10.1016/j.compositesa.2014.08.027>
- [6] Swolfs Y, Verpoest I, Gorbatiikh L. Recent advances in fibre-hybrid composites: materials selection, opportunities and applications. *Int Mater Rev* 2019;64:181–215.  
<https://doi.org/10.1080/09506608.2018.1467365>
- [7] Czél G, Jalalvand M, Wisnom MR, Czigány T. Design and characterisation of high performance, pseudo-ductile all-carbon/epoxy unidirectional hybrid composites. *Compos Part B Eng* 2017;111:348–56. <https://doi.org/10.1016/j.compositesb.2016.11.049>
- [8] Suwarta P, Czél G, Fotouhi M, Rycerz J, Wisnom MR. Pseudo-ductility of unidirectional thin ply hybrid composites in longitudinal compression. *33rd Tech. Conf. Am. Soc. Compos.* 2018, vol. 2, 2018, p. 1032–41. <https://doi.org/10.12783/asc33/25987>
- [9] Wu X, Wisnom MR. Compressive Failure Strain of Unidirectional Carbon Fibre Composites from Bending Tests. *Compos Struct* 2022;304:116467.  
<https://doi.org/10.1016/j.compstruct.2022.116467>
- [10] Czél G, Jalalvand M, Wisnom MR. Hybrid specimens eliminating stress concentrations in tensile and compressive testing of unidirectional composites. *Compos Part A Appl Sci Manuf* 2016;91:436–47. <https://doi.org/10.1016/j.compositesa.2016.07.021>
- [11] Wisnom MR. Size effects in the testing of fibre-composite materials. *Compos Sci Technol* 1999;59:1937–57. [https://doi.org/10.1016/S0266-3538\(99\)00053-6](https://doi.org/10.1016/S0266-3538(99)00053-6)
- [12] Suwarta P. Pseudo-ductility of Unidirectional Thin-Ply Hybrid Composites. University of Bristol, 2020.
- [13] Clauß S, Pescatore C, Niemz P. Anisotropic elastic properties of common ash (*Fraxinus excelsior* L.). *Holzforschung* 2014;68:941–9. <https://doi.org/10.1515/hf-2013-0189>
- [14] Knorz M, Schmidt M, Torno S, Van De Kuilen JW. Structural bonding of ash (*Fraxinus excelsior* L.): Resistance to delamination and performance in shearing tests. *Eur J Wood Wood Prod* 2014;72:297–309. <https://doi.org/10.1007/s00107-014-0778-8>
- [15] Montagnier O, Hochard C. Compression characterization of high-modulus carbon fibers. *J Compos Mater* 2005;39:35–49. <https://doi.org/10.1177/0021998305046>